Exploration of Victoria Crater by the Mars Rover Opportunity

S. W. Squyres, *et al.*

Science **324**, 1058 (2009);
DOI: 10.1126/science.1170355

Exploration of Victoria Crater by the Mars Rover Opportunity

S. W. Squyres,[1]* A. H. Knoll,[2] R. E. Arvidson,[3] J. W. Ashley,[4] J. F. Bell III,[1] W. M. Calvin,[5] P. R. Christensen,[4] B. C. Clark,[6] B. A. Cohen,[7] P. A. de Souza Jr.,[8] L. Edgar,[9] W. H. Farrand,[10] I. Fleischer,[11] R. Gellert,[12] M. P. Golombek,[13] J. Grant,[14] J. Grotzinger,[9] A. Hayes,[9] K. E. Herkenhoff,[15] J. R. Johnson,[15] B. Jolliff,[3] G. Klingelhöfer,[11] A. Knudson,[4] R. Li,[16] T. J. McCoy,[17] S. M. McLennan,[18] D. W. Ming,[19] D. W. Mittlefehldt,[19] R. V. Morris,[19] J. W. Rice Jr.,[4] C. Schröder,[11] R. J. Sullivan,[1] A. Yen,[13] R. A. Yingst[20]

The Mars rover Opportunity has explored Victoria crater, a ~750-meter eroded impact crater formed in sulfate-rich sedimentary rocks. Impact-related stratigraphy is preserved in the crater walls, and meteoritic debris is present near the crater rim. The size of hematite-rich concretions decreases up-section, documenting variation in the intensity of groundwater processes. Layering in the crater walls preserves evidence of ancient wind-blown dunes. Compositional variations with depth mimic those ~6 kilometers to the north and demonstrate that water-induced alteration at Meridiani Planum was regional in scope.

The Mars Exploration Rover Opportunity examined a small bedrock outcrop at its landing site in Eagle crater (*1*) and ~7.5 m of stratigraphy at Endurance crater, 800 m to the east (*2*). Here, we report on a third stratigraphic section, more than 10 m thick, at Victoria crater, 6 km south of Eagle and Endurance.

Exploration of Victoria (Fig. 1) began on sol 952 (*3*) with a traverse along the crater's northern rim, imaging cliff faces to document stratigraphy. Opportunity then drove to Duck Bay and descended into the crater on sol 1293 to begin in situ observations. Opportunity exited the crater on sol 1634.

Victoria crater is ~750 m in diameter and ~75 m deep. Its outline is serrated, with sharp, steep promontories separated by rounded, less steep alcoves. The crater rim is ~4 to 5 m high and ~120 to 220 m wide. It is surrounded by an annulus of smooth terrain that extends approximately one crater diameter from the rim, suggesting that the annulus is derived from the crater's ejecta blanket. Such characteristics, along with observed morphology and ejecta thickness, indicate that Victoria formed as a primary crater ~600 m in diameter and ~125 m deep (*4*). On the crater floor is a dune field. The crater has been widened by erosion, and its depth has been reduced by deposition of wind-blown sand and material released from the crater walls. Eolian erosion and mass wasting have contributed to the development of alcoves and promontories.

The sulfate-rich sedimentary rocks at Meridiani are easily eroded by eolian abrasion (*1*, *2*). Therefore, the annulus, although derived from the original ejecta blanket, preserves no perched ejecta blocks; they have been planed off by eolian abrasion. Ejecta currently is exposed only in the uppermost interior walls of the crater and near the rim where soil cover is discontinuous. There is no evidence that the impact excavated through the sediments into an underlying nonsedimentary basement unit.

Small hematite-rich spherules interpreted as concretions characterize sedimentary rocks throughout Meridiani (*1*, *2*). Opportunity gained more than 30 m of elevation during the traverse from Endurance to Victoria; because regional outcrop is approximately flat-lying, this may have been a traverse up-section. Spherule size observed in outcrop shows a systematic decrease with elevation (*5*–*7*) (fig. S1), documenting regional and/or stratigraphic variation in the intensity of groundwater processes (e.g., less water higher in the section) after sulfate-rich sand deposition.

Once Opportunity entered Victoria's annulus, large spherules reappeared in the soil. The source of these spherules is suggested by ejecta blocks at the Cape of Good Hope that exhibit purple-gray colors in Pancam (*8*) false-color views (*9*), distinct from typical outcrop rocks (Fig. 2). Pancam spectra of these blocks are correspondingly unusual, exhibiting negative 754- to 1009-nm slopes and weaker 535-nm band depths than typical "purple" rocks (*10*). We chose one, Cercedilla, for study, which unlike nearby bedrock contains large (~6 mm) spherules.

Cercedilla was abraded using the Rock Abrasion Tool (RAT) (*11*) (Fig. 2c) and imaged with the Microscopic Imager (MI) (*12*). The elemental chemistry of Cercedilla revealed by the Alpha Particle X-Ray Spectrometer (APXS) (*13*) is similar to that in the deepest part of Endurance crater (*14*) and is distinct from that in the examined section in Victoria crater, in having lower FeO_T/Al_2O_3 (where FeO_T is total iron expressed as FeO) and no Cl enrichment.

[1]Department of Astronomy, Space Sciences Building, Cornell University, Ithaca, NY 14853, USA. [2]Botanical Museum, Harvard University, Cambridge, MA 02138, USA. [3]Department of Earth and Planetary Sciences, Washington University, St. Louis, MO 63031, USA. [4]School of Earth and Space Exploration, Arizona State University, Tempe, AZ 85287, USA. [5]University of Nevada, Reno, Geological Sciences, Reno, NV 89557, USA. [6]Lockheed Martin Corporation, Littleton, CO 80127, USA. [7]National Aeronautics and Space Administration, Marshall Space Flight Center, Huntsville, AL 35812, USA. [8]Tasmanian Information and Communication Technologies Centre, Commonwealth Scientific and Industrial Research Organisation, Castray Esplanade, Hobart TAS 7000, Australia. [9]Division of Geological and Planetary Sciences, California Institute of Technology, Pasadena, CA 91125, USA. [10]Space Science Institute, Boulder, CO 80301, USA. [11]Institut für Anorganische und Analytische Chemie, Johannes Gutenberg-Universität, Mainz, Germany. [12]Department of Physics, University of Guelph, Guelph, ON, N1G 2W1, Canada. [13]Jet Propulsion Laboratory, California Institute of Technology, Pasadena, CA 91109, USA. [14]Center for Earth and Planetary Studies, Smithsonian Institution, Washington, DC 20560, USA. [15]U.S. Geological Survey, Flagstaff, AZ 86001, USA. [16]Department of Civil and Environmental Engineering and Geodetic Science, Ohio State University, Columbus, OH 43210, USA. [17]Department of Mineral Sciences, National Museum of Natural History, Smithsonian Institution, Washington, DC 20560, USA. [18]Department of Geosciences, State University of New York, Stony Brook, NY 11794, USA. [19]Astromaterials Research and Exploration Science, NASA Johnson Space Center, Houston, TX 77058, USA. [20]Natural and Applied Sciences, University of Wisconsin Green Bay, Green Bay, WI 54311, USA.

*To whom correspondence should be addressed. E-mail: squyres@astro.cornell.edu

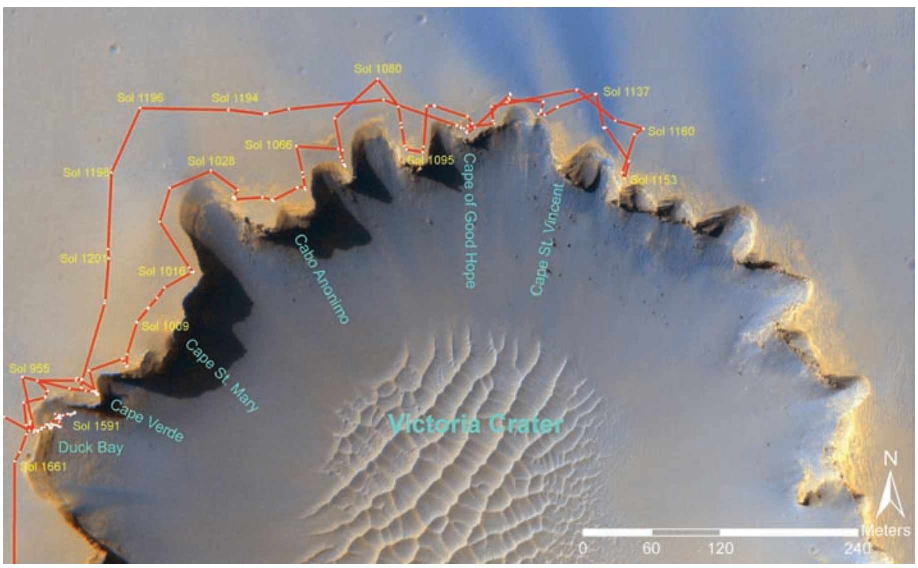

Fig. 1. Opportunity's traverse at Victoria crater. Image acquired by the Mars Reconnaissance Orbiter High Resolution Imaging Science Experiment camera.

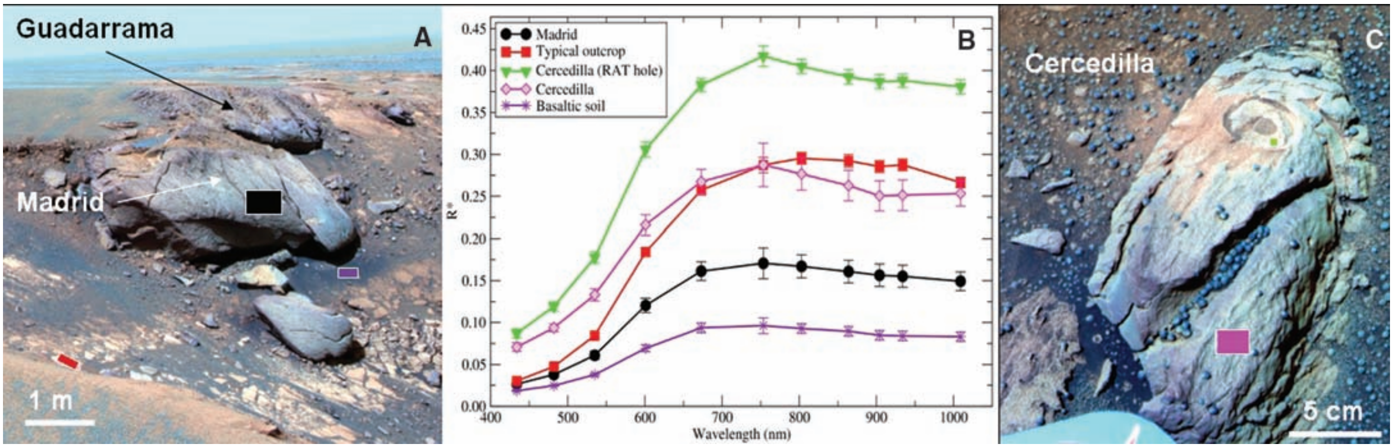

Fig. 2. (**A**) Pancam false-color image (red, 753 nm; green, 535 nm; blue, 432 nm) of Madrid and Guadarrama (sequence p2579, sol 1097). (**B**) Pancam spectra [R^* = absolute reflectivity/cos(incidence angle)] of regions outlined in (A) and (C). (**C**) Pancam false-color image of Cercedilla (sequence p2564, sol 1184).

Cercedilla and other spectrally similar blocks probably represent materials excavated during crater formation from a deeper stratigraphic unit within Victoria crater. The abundance of large spherules in Cercedilla supports the idea that the spherules in the annulus were released by erosion from deeply sourced, spherule-rich ejecta, consistent with the hypothesis that the systematic decrease in spherule size from Endurance to Victoria reflects stratigraphic variation.

As Opportunity drove south toward Victoria, large eolian ripples became prominent as mean spherule size declined. The Victoria annulus is covered by large spherules eroded from ejecta and lacks large ripples, which suggests that accumulations of larger spherules create dense, protective lags that impede eolian transport, stabilizing the soil and inhibiting ripple development.

Opportunity encountered a field of loose rocks at Cabo Anonimo. All have similar Pancam spectral properties, including absorption features consistent with the presence of olivine and/or low-Ca pyroxene. Miniature Thermal Emission Spectrometer (Mini-TES) (*15*) spectra of the 12 rocks observed are also similar to one another; together these observations imply a common composition for all the rocks in the field.

One of the largest rocks, Santa Catarina (~11 by 14 cm), was chosen for detailed analysis. MI images show brecciation, with some clasts exhibiting possible igneous quench textures (fig. S2). Mössbauer (*16*) spectra confirm olivine and pyroxene and reveal troilite. The elemental chemistry of Santa Catarina is unusual for Meridiani but closely approximates that of Barberton (*17*), a pebble at the rim of Endurance crater. Kamacite, an iron-nickel alloy, was identified in Barberton, which suggests that it is a meteorite. Its composition is consistent with a mesosiderite silicate clast (*17*). We infer that Santa Catarina and the other rocks in the field on Cabo Anonimo are also meteoritic. Presumably, they are better preserved than the friable ejecta blocks because their achondritic composition makes them more resistant to erosion. Troilite is more abundant than metal in silicate clasts of the Vaca Muerta mesosiderite (*18*), and some troilite in Santa Catarina may have remained while the metal phase was altered [although alteration may have required several hundred million years of water exposure (*19*)]. Santa Catarina Mössbauer spectra reveal proportionally more ferric iron than in Barberton, which may indicate greater alteration. Alternatively, Santa Catarina may contain kamacite clasts that went undetected because of heterogeneity in the breccia. Santa Catarina and Barberton may be related, because mesosiderites are rare and these rocks were found within a few kilometers of one another. Santa Catarina and nearby rocks may be fragments of the impactor that created Victoria crater.

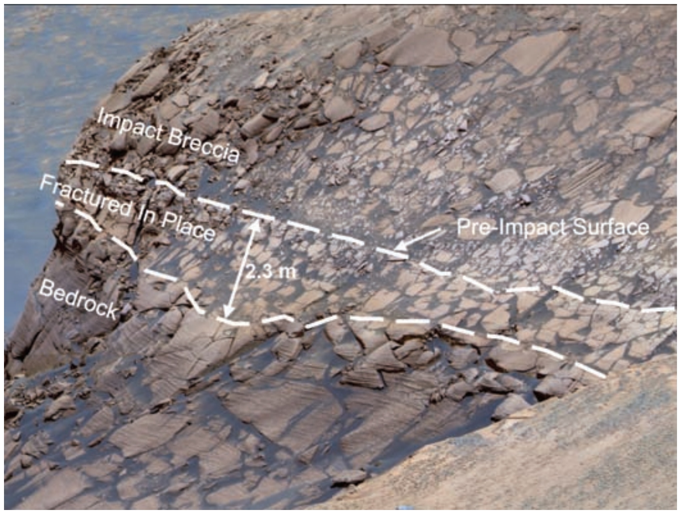

Fig. 3. Pancam false-color image of the east face of Cape Verde, showing typical impact-related stratigraphy (sequence p2429, sol 1006).

The lowest materials in the crater walls are intact bedrock (Fig. 3). These beds grade upward into rock that is fractured but in place, as shown by bedding planes that retain their original orientation. The fracturing probably took place during the impact, as the shock wave impinged on the free surface, loading rocks in tension. Immediately above the pre-impact surface is an abrupt transition to ejecta blocks with bedding planes in random orientations.

The crater walls exhibit distinctive horizontal color and albedo banding immediately below the pre-impact surface (fig. S3). The uppermost unit (Steno) has a blue-to-red slope and a 535-nm band depth that are low compared with the underlying unit (Smith). The color properties of these units are similar, respectively, to darker-toned and lighter-toned rocks observed elsewhere at Meridiani (*10*). The next lower unit (Lyell) is spectrally similar to Steno. This color sequence was also observed at Endurance crater (*10*).

Cape St. Mary, Cape St. Vincent, and Cape Verde were imaged from the crater rim using techniques that combine information from multiple images (*20*) to enhance resolution. The three promontories are dominated by eolian facies. No clasts are visible at Pancam resolution, consistent with the exclusively sand-sized grains in all outcrops observed by Opportunity. Bedding is clearly distinguishable everywhere. Meter-scale eolian cross-stratification is visible in several promontories, including Cape St. Mary and Cape St. Vincent (Fig. 4). Elsewhere bedding is massive, planar, or observed as low-angle climbing translatent cross-strata.

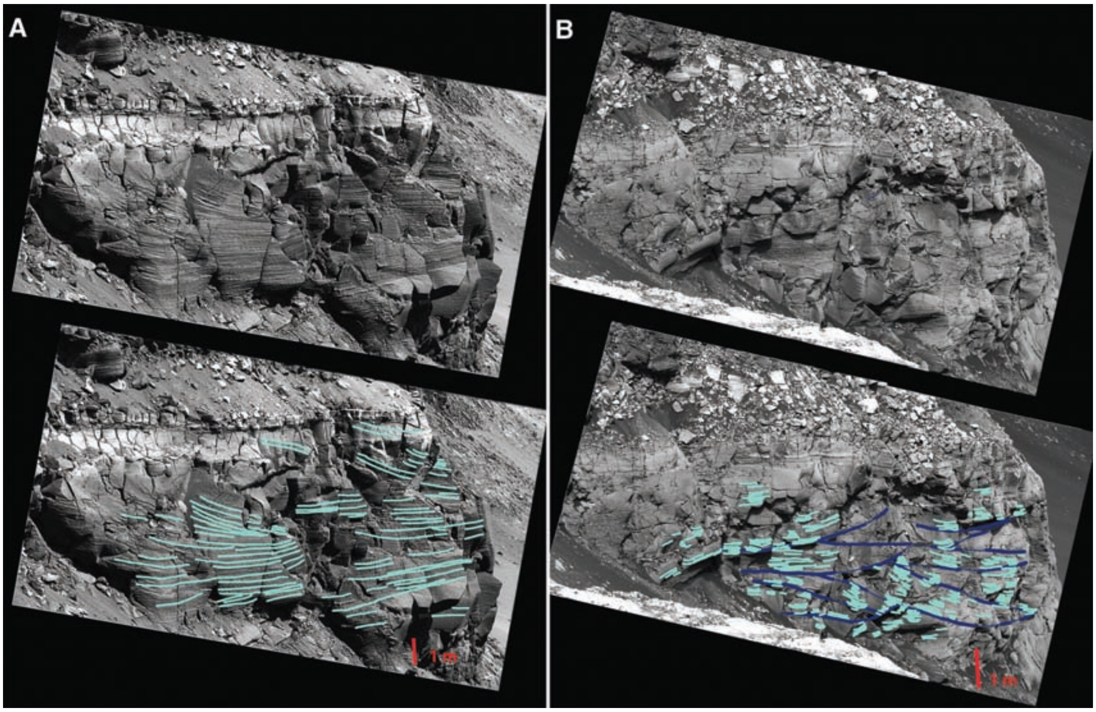

Fig. 4. Pancam images of Cape St. Vincent (**A**), sequence p2417, sol 1167, and Cape St. Mary (**B**), sequence p2444, sol 1213. Lower images have bedding and cross-stratification highlighted.

Cape St. Vincent presents a west-facing outcrop dominated by an 8-m vertical exposure of large-scale cross-strata. The stratification suggests subcritical climbing bedforms with decameter-scale dune heights that migrated approximately parallel to the outcrop face. Color and albedo banding below the pre-impact surface is prominent. The banding is nearly horizontal and cut by bedding at a high angle, so it is diagenetic in origin rather than a primary depositional feature.

Cape St. Mary presents a south-facing outcrop dominated by a 6-m vertical exposure of meter-scale sets of trough cross-bedding (bedding concordant with set boundaries). This layering is indicative of decameter-scale, sinuous-crested, eolian dunes that migrated approximately perpendicular to the outcrop face. No erosional contacts are observed.

Cape Verde shows evidence for an erosional contact at its base (fig. S4). The lowermost unit is dominated by thickly bedded dune toeset laminae. Evidence for diagenesis at Cape Verde includes truncated and cross-cutting facture fills, preferentially eroded bedding, and a ribbed weathering pattern superimposed on cross-strata, suggesting differential cementation.

The cross-stratification at Victoria is comparable in scale (several meters) to Jurassic eolian deposits of the western United States, implying a dry dune field. The grain size, scale, angle of exposed bedding, and lack of volcanic bombs or other outsized clasts are inconsistent with a pyroclastic or impact origin (*21*, *22*).

Opportunity performed in situ observations of the Steno, Smith, and Lyell units at Duck Bay. All are sulfate-rich sandstone. Steno has a vertical thickness of ~70 cm and is fine-to-medium-grained, with well-defined laminae. Centimeter-to-meter–scale cross-bedding is visible, and spherules are abundant. Steno and Smith are separated by a low-angle disconformity. Smith has a vertical thickness of ~80 cm and is smoother and lighter-toned than Steno and Lyell, with fine planar laminations.

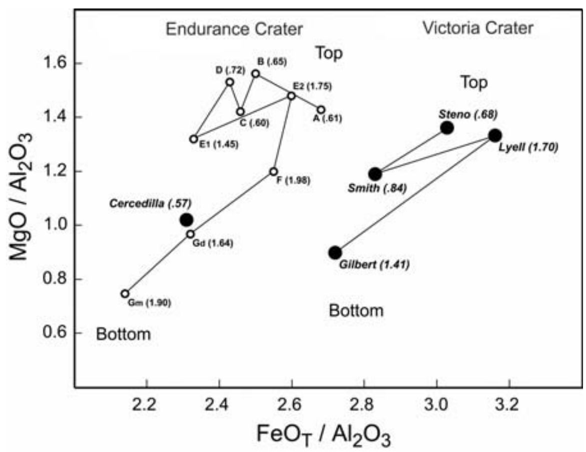

Fig. 5. Plot of MgO/Al_2O_3 versus FeO_T/Al_2O_3 for abraded targets from Endurance crater (open circles) and Victoria crater (closed circles). Samples are joined in stratigraphic order. Cl concentrations in weight percent are in parentheses.

The Smith-Lyell contact is gradational. Lyell is darker than Smith because of basaltic sand trapped in surface porosity. It is a well-sorted, fine-grained sandstone with a vertical thickness of 1.85 m, prominent millimeter-to-centimeter–scale laminations, and cross-bed sets up to several meters thick. Spherules are more common than in Smith and Steno. The porosity comes partly from tabular prismatic vugs, similar to those at Eagle crater (*23*).

Elemental compositions at Duck Bay (Fig. 5) fall mostly within established ranges for Meridiani, but with more Fe; the lowermost unit investigated (Gilbert, immediately below Lyell) has more Fe than previously measured in Meridiani bedrock. Other elements commonly associated with Fe, including Ti, Mn, Cr, and Ni, display no enhancements. All rocks are sulfate-rich; Steno has more S than previously observed at Meridiani.

Higher Fe aside, stratigraphic trends in outcrop chemistry compare closely to those at Endurance. Both sections show down-section decreases in S, Fe, and Mg, and corresponding Al and Si enrichment. Both also show a sharp discontinuity in Cl content; lower parts of the sections at both craters are 2 to 3 times as high as uppermost units. At Duck Bay, the main chemical discontinuity coincides with the Smith-Lyell contact, likely corresponding to a diagenetic boundary. Cl discontinuities occur slightly above the level at which decreases in MgO/Al_2O_3 and FeO_T/Al_2O_3 begin (Fig. 5).

Measured sections at Endurance and Victoria are similar in character but differ in detail, consistent with the hypothesis that Victoria rocks lie stratigraphically above those at Endurance. On the basis of cross-cutting relationships, textural features at Endurance crater suggest relatively late diagenetic events (*24*) that record chemical interaction with a local groundwater table (*21*, *24*). If correct, the observation of comparable vertical trends in sections that may represent distinct stratigraphic levels could imply that a set of depositional and early diagenetic processes recurred through time during regional stratigraphic development. Alternatively, chemostratigraphic trends at Endurance may reflect downward-penetrating diagenesis related to surface exposure (*25*). This would allow chemical trends in both sections to reflect a single alteration event that took place during or after development of the current land surface. In either case, the wettest conditions occurred during deposition and early diagenesis, with drying thereafter (*26*).

Opportunity's investigation of Victoria crater shows that depositional, diagenetic, and erosional processes documented locally at Eagle and Endurance craters acted regionally. These processes include (i) chemical interaction of basalts and acidic water to produce sulfate salts; (ii) production of sands, transport and deposition by wind, and subsequent groundwater-influenced cementation; (iii) later diagenetic alteration of outcrop surfaces under increasingly arid conditions; and (iv) erosion of friable sedimentary rocks by persistent wind action, continuing to the present.

References and Notes

1. S. W. Squyres *et al*., *Science* **306**, 1698 (2004).
2. S. W. Squyres *et al*., *Science* **313**, 1403 (2006).
3. A sol is defined as one martian solar day.
4. J. A. Grant *et al*., *J. Geophys. Res.* **113**, E11010; 10.1029/2008JE003155 (2008).
5. C. Weitz *et al*., *J. Geophys. Res.* **111**, E12S04; 10.1029/2005JE002541 (2006).
6. W. M. Calvin *et al*., *J. Geophys. Res.* **113**, E12S37; 10.1029/2007JE003048 (2008).
7. K. E. Herkenhoff *et al*., *J. Geophys. Res.* **113**, E12S32; 10.1029/2008JE003100 (2008).
8. J. F. Bell III *et al*., *J. Geophys. Res.* **108**, 8063; 10.1029/2003JE002070 (2003).
9. Colors based on contrast-stretched red-green-blue composites from Pancam's 673-, 535-, and 432-nm filters.
10. W. H. Farrand *et al*., *J. Geophys. Res.* **112**, E06S02; 10.1029/2006JE002773 (2007).
11. S. Gorevan *et al*., *J. Geophys. Res.* **108**, 8068; 10.1029/2003JE002061 (2003).
12. K. E. Herkenhoff *et al*., *J. Geophys. Res.* **108**, 8065; 10.1029/2003JE002076 (2003).
13. R. Rieder *et al*., *J. Geophys. Res.* **108**, 8066; 10.1029/2003JE002150 (2003).
14. B. C. Clark *et al*., *Earth Planet. Sci. Lett.* **240**, 73 (2005).
15. P. R. Christensen *et al*., *J. Geophys. Res.* **108**, 8064; 10.1029/2003JE002117 (2003).
16. G. Klingelhöfer *et al*., *J. Geophys. Res.* **108**, 8067; 10.1029/2003JE002138 (2003).
17. C. Schröder *et al*., *J. Geophys. Res.* **113**, E06S22; 10.1029/2007JE002990 (2008).
18. M. Kimura *et al*., *Proc. NIPR Symp. Antarct. Meteorites* **4**, 263 (1991).
19. P. A. Bland, T. B. Smith, *Icarus* **144**, 21 (2000).
20. J. F. Bell III *et al*., *J. Geophys. Res.* **111**, E02S03; 10.1029/2005JE002444 (2006).
21. J. P. Grotzinger *et al*., *Earth Planet. Sci. Lett.* **240**, 11 (2005).
22. K. E. Herkenhoff *et al*., *J. Geophys. Res.* **113**, E12S32; 10.1029/2008JE003100 (2008).
23. S. W. Squyres *et al*., *Science* **306**, 1709 (2004).
24. S. M. McLennan *et al*., *Earth Planet. Sci. Lett.* **240**, 95 (2005).
25. R. Amundson *et al*., *Geochim. Cosmochim. Acta* **72**, 3845 (2008).
26. A. H. Knoll *et al*., *J. Geophys. Res.* **113**, E06S16; 10.1029/2007JE002949 (2008).

27. This research was carried out for the Jet Propulsion Laboratory, California Institute of Technology, under a contract with NASA.

Supporting Online Material

www.sciencemag.org/cgi/content/full/324/5930/1058/DC1
Figs. S1 to S4

29 December 2008; accepted 31 March 2009
10.1126/science.1170355

Bone Assemblages Track Animal Community Structure over 40 Years in an African Savanna Ecosystem

David Western[1] and Anna K. Behrensmeyer[2]

Reconstructing ancient communities depends on how accurately fossil assemblages retain information about living populations. We report a high level of fidelity between modern bone assemblages and living populations based on a 40-year study of the Amboseli ecosystem in southern Kenya. Relative abundance of 15 herbivorous species recorded in the bone assemblage accurately tracks the living populations through major changes in community composition and habitat over intervals as short as 5 years. The aggregated bone sample provides an accurate record of community structure time-averaged over four decades. These results lay the groundwork for integrating paleobiological and contemporary ecological studies across evolutionary and ecological time scales. Bone surveys also provide a useful method of assessing population changes and community structure for modern vertebrates.

Accurate reconstructions of ancient community ecology depend on how closely fossil assemblages match species richness and relative abundances in the original living communities. Many taphonomic and methodological biases relating to morphology, body size, and life habit can affect the presence or absence of taxa and their relative abundance in fossil assemblages (*1*–*4*). Vertebrates and shelly invertebrates have durable remains that can accumulate over long periods of time, raising questions about how such remains record properties of the original community, especially during periods of marked population and habitat change (*2*–*5*). Data quality issues have been addressed through studies of living populations and their death assemblages in marine invertebrates (*3*, *4*, *6*, *7*) and terrestrial vertebrates (*8*–*10*). These "live:dead" studies show that single-census death assemblages can approximate ecological snapshots but typically include durable remains representing varying intervals of accumulation, or time averaging. Time averaging usually inflates species richness relative to live samples, but under stable population and environmental conditions can accurately represent rank abundances of the dominant species in shelly invertebrate assemblages (*3*, *4*, *6*, *7*).

Earlier, single-census live:dead research in the Amboseli ecosystem demonstrated preburial fidelity of the surface bone assemblage with respect to large (15 to 4000 kg) herbivore populations and their habitat distributions (*8*, *11*–*13*). Birth and death rates among species, and hence the production of skeletal remains, are inversely scaled to species body weight (*12*). Consequently, the greater numbers of dead smaller animals were offset by allometrically scaled bone destruction

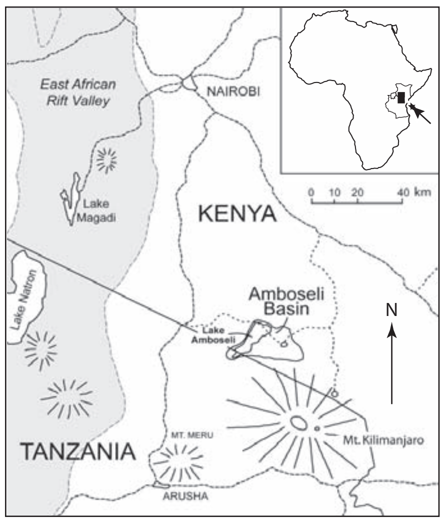

Fig. 1. Regional map of southern Kenya showing the physiographic context of the Amboseli Basin north of Mount Kilimanjaro. Lake Amboseli is a shallow, seasonal playa with wetlands fed by springs from Mount Kilimanjaro.

[1]African Conservation Center, Box 62844, Nairobi, Kenya. [2]Department of Paleobiology, MRC 121, National Museum of Natural History, Smithsonian Institution, Post Office Box 37012, Washington, DC 20013–7012, USA.

E-mail: dwestern@africaonline.co.ke (D.W.); behrensa@si.edu (A.K.B.)